Electronic Supplementary Material (ESI) for Journal of Materials Chemistry C.


Electronic Supplementary Material (ESI) for Journal of Materials Chemistry C.

# Electronic Supplementary Information

**Tert-butyl Substituted Hetero-donor TADF compounds for Efficient Solution-Processed Non-doped Blue OLEDs**

Feng-Ming Xie,[†,a] Zhi-Dong An,[†,a] Miao Xie,[a] Yan-Qing Li,*[,a,b] Guang-Hui Zhang,[a] Shi-Jie Zou,[a] Li Chen,[a] Jing-De Chen,[a] Tao Cheng,*[,a] and Jian-Xin Tang*[,a,c]

[a] *Jiangsu Key Laboratory for Carbon-Based Functional Materials & Devices, Institute of Functional Nano & Soft Materials (FUNSOM), Soochow University, Suzhou, Jiangsu 215123, China*

[b] *School of Physics and Electronics Science, Ministry of Education Nanophotonics & Advanced Instrument Engineering Research Center, East China Normal University, Shanghai, 200062, China*

[c] *Institute of Organic Optoelectronics (IOO), JITRI, Wujiang, Suzhou 215215, China*

* E-mail: yqli@suda.edu.cn (Y.Q. Li), tcheng@suda.edu.cn (T. Cheng), jxtang@suda.edu.cn (J.X. Tang)

† These authors contribute equally to this work.

**2Cz2tCzBn:** $^{1}$H NMR (400 MHz, $CDCl_3$) δ 8.36 (s, 1H), 7.71-7.68 (m, 8H), 7.20 (d, *J* = 8.2 Hz, 8H), 7.14 (dd, *J* = 8.6, 1.7 Hz, 4H), 7.10-7.02 (m, 8H), 1.35 (s, 36H). $^{13}$C NMR (101 MHz, $CDCl_3$) δ 144.12, 139.33, 138.77, 137.46, 137.11, 135.72, 125.43, 124.50, 123.88, 123.14, 120.68, 119.86, 118.10, 116.16, 113.43, 109.59, 109.29, 34.59, 31.83. MS (APCI) calcd. for $C_{71}H_{65}N_5$: m/z = 987.52, found: 1005.6 $[M+18]^+$.

**2PhCz2tCzBn:** $^{1}$H NMR (400 MHz, $CDCl_3$) δ 8.50 (s, 1H), 7.96 (s, 4H), 7.70 (s, 4H), 7.60 (d, *J* = 7.6 Hz, 8H), 7.46 (t, *J* = 7.6 Hz, 8H), 7.38-7.32 (m, 6H), 7.31 (s, 4H), 7.28 (d, *J* = 3.6 Hz, 2H), 7.25 (s, 4H), 7.19 (dd, *J* = 8.7, 1.0 Hz, 4H), 1.35 (s, 36H). $^{13}$C NMR (101 MHz, $CDCl_3$) δ 144.30, 141.52, 139.29, 138.82, 137.50, 136.79, 135.71, 134.44, 128.77, 127.16, 126.77, 125.12, 124.69, 124.57, 123.28, 118.37, 116.23, 109.74, 109.71, 34.62, 31.84. MS (APCI) calcd. for $C_{95}H_{81}N_5$: m/z = 1292.65, found: 1310.7 $[M+18]^+$.

**2tCz2PhCzBn:** $^{1}$H NMR (400 MHz, $CDCl_3$) δ 8.49 (s, 1H), 7.98 (s, 4H), 7.71 (d, *J* = 1.5 Hz, 4H), 7.61 (d, *J* = 7.4 Hz, 8H), 7.47 (t, *J* = 7.6 Hz, 8H), 7.41-7.33 (m, 13H), 7.23 (s, 1H), 7.21 (s, 2H), 7.14 (dd, *J* = 8.6, 1.7 Hz, 4H), 1.35 (s, 36H). $^{13}$C NMR (101 MHz, $CDCl_3$) δ 144.13, 141.63, 139.01, 137.82, 137.34, 134.74, 128.74, 127.24, 126.73, 125.26, 125.02, 124.22, 123.26, 118.58, 116.12, 110.51, 108.93, 34.61, 31.82. MS (APCI) calcd. for $C_{95}H_{81}N_5$: m/z = 1292.65, found: 1310.7 $[M+18]^+$.

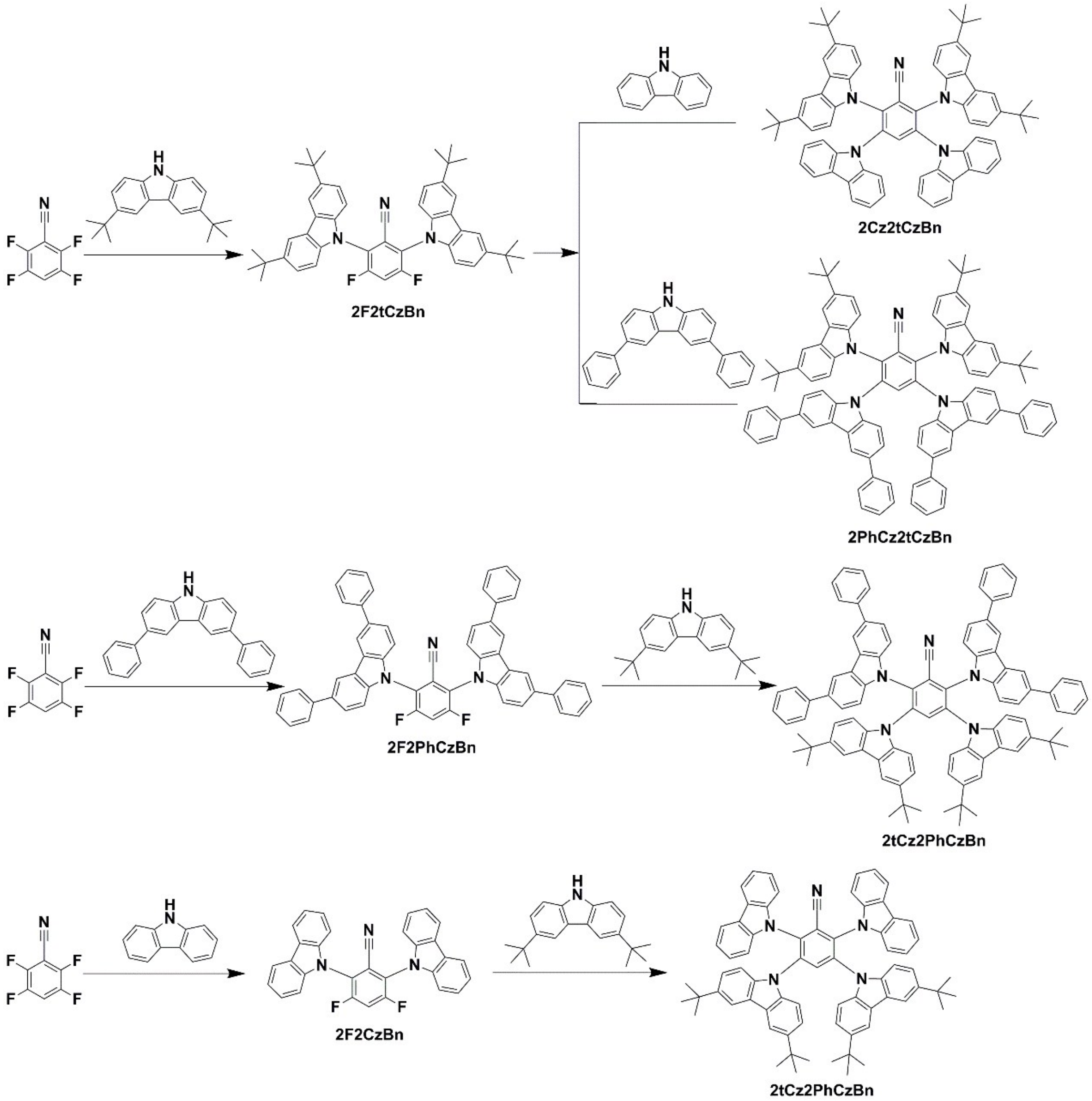


**Scheme S1**. Synthetic routes of **2Cz2tCzBn**, **2tCz2CzBn**, **2PhCz2tCzBn**, and **2tCz2PhCzBn**, respectively.

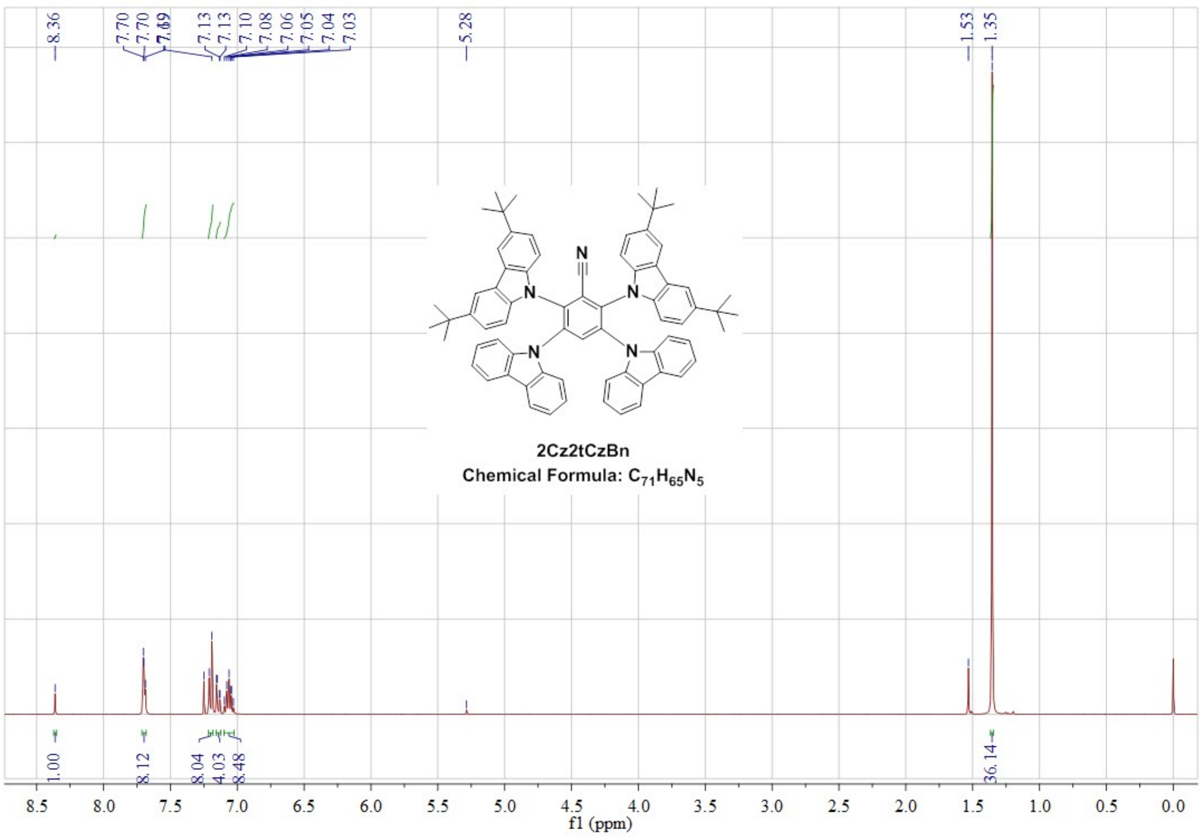


**Figure S1.** $^1$H NMR spectrum of 2Cz2tCzBn.

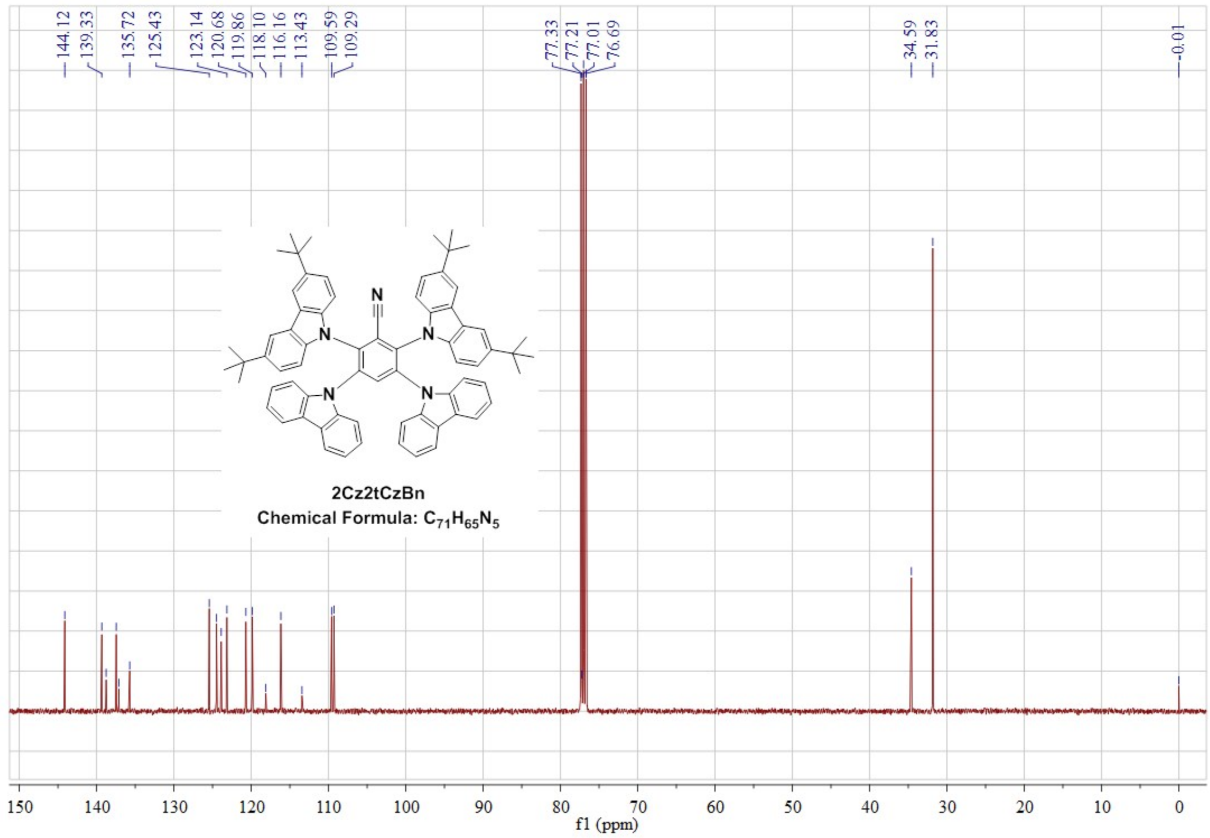


**Figure S2.** $^{13}$C NMR spectrum of 2Cz2tCzBn.

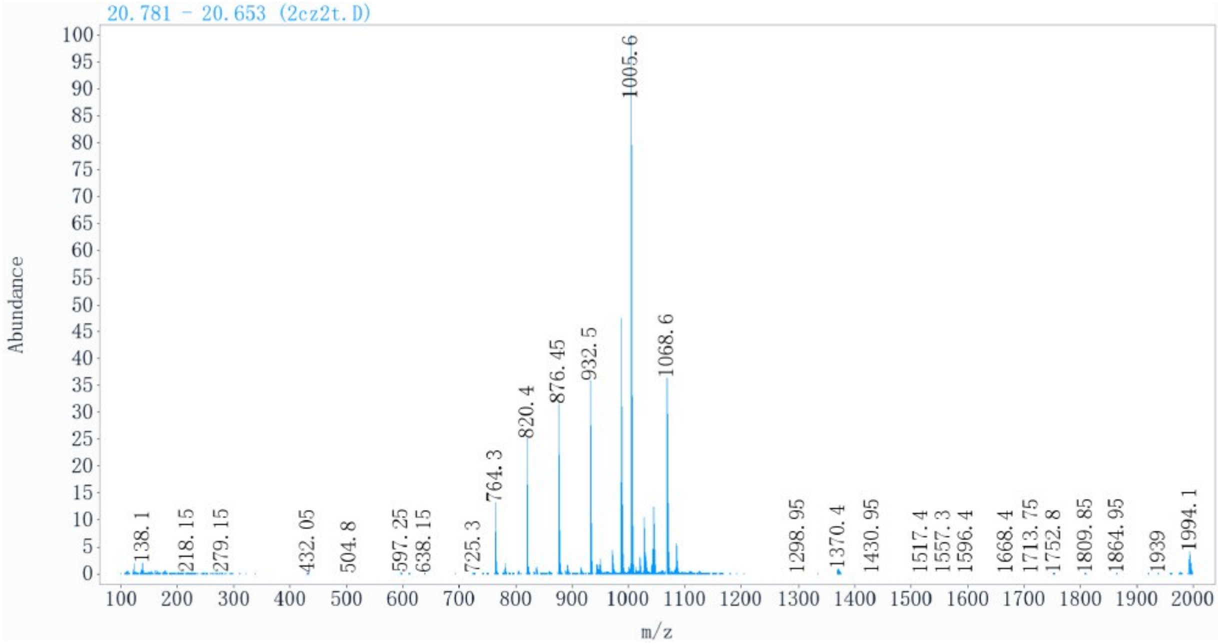


**Figure S3.** TOF-MS spectrum of 2Cz2tCzBn.

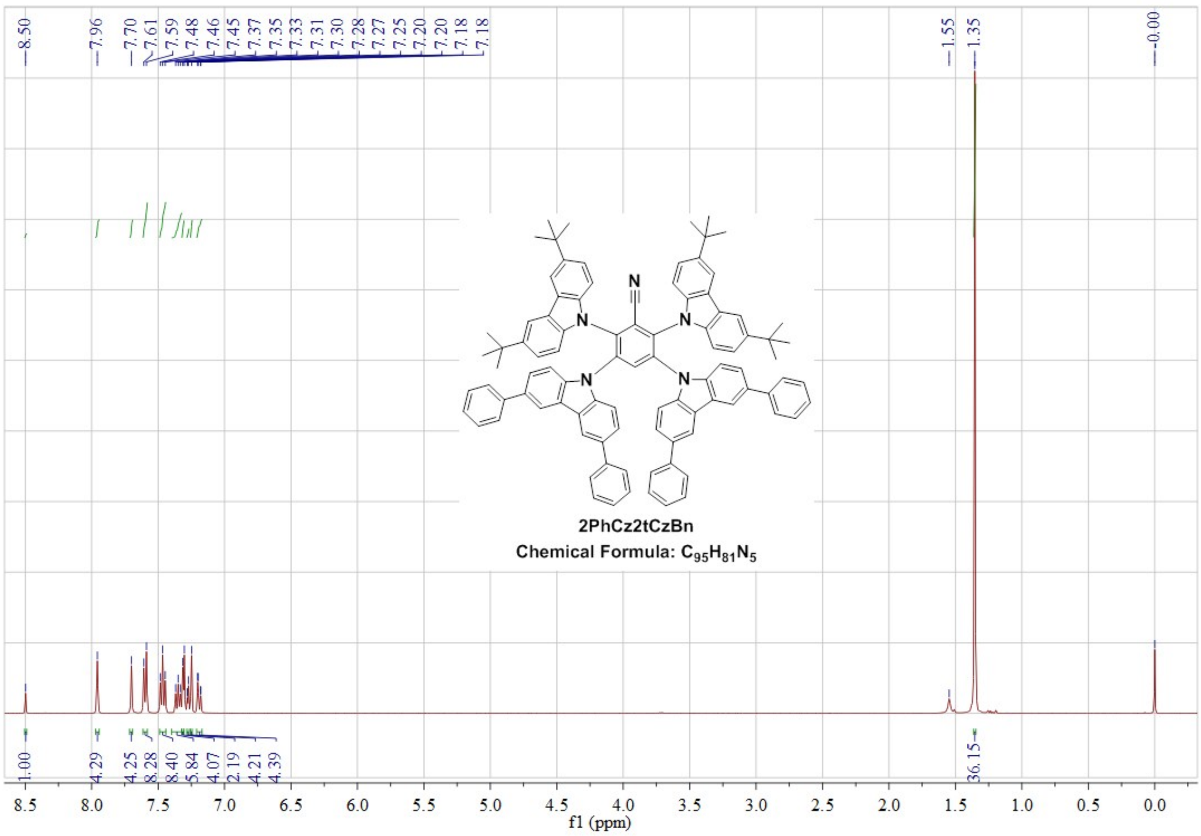


**Figure S4.** $^{1}$H NMR spectrum of 2PhCz2tCzBn.

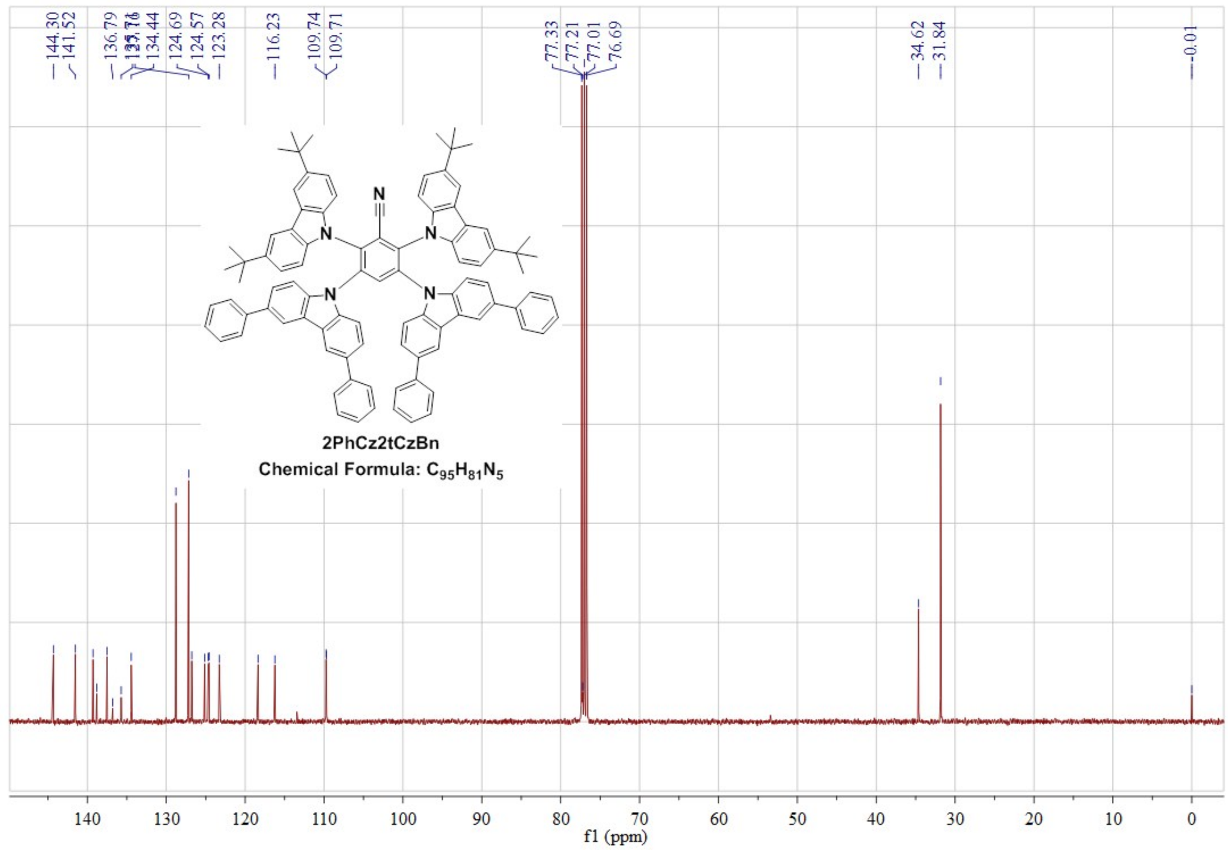


**Figure S5.** $^{13}C$ NMR spectrum of 2PhCz2tCzBn.

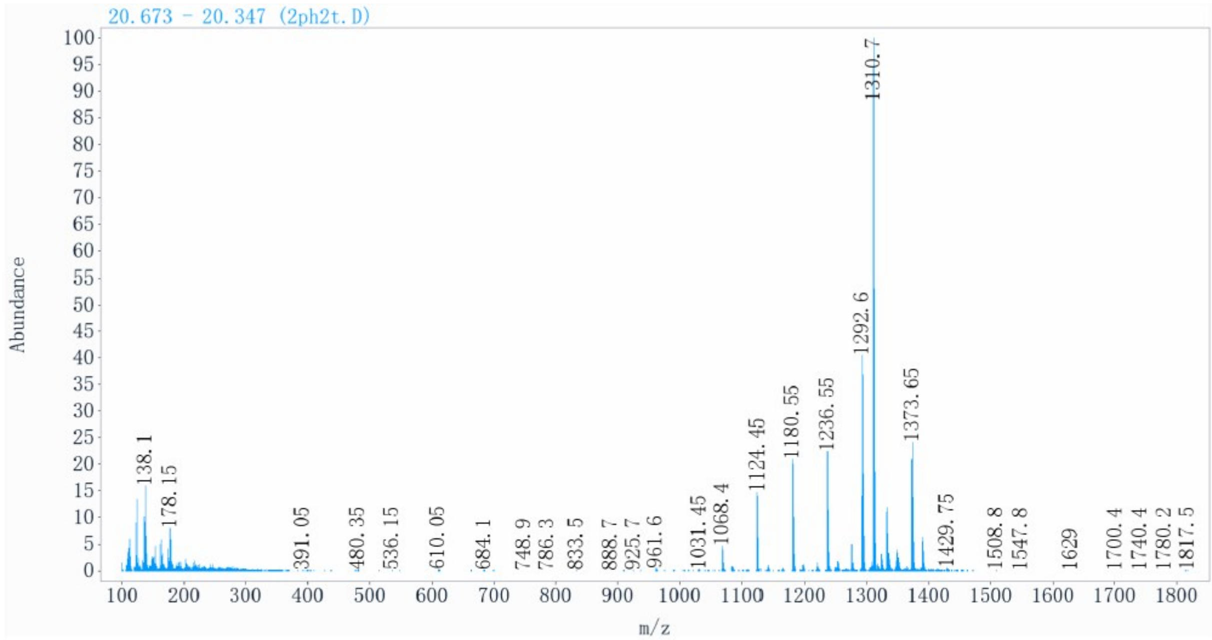


**Figure S6.** TOF-MS spectrum of 2PhCz2tCzBn.

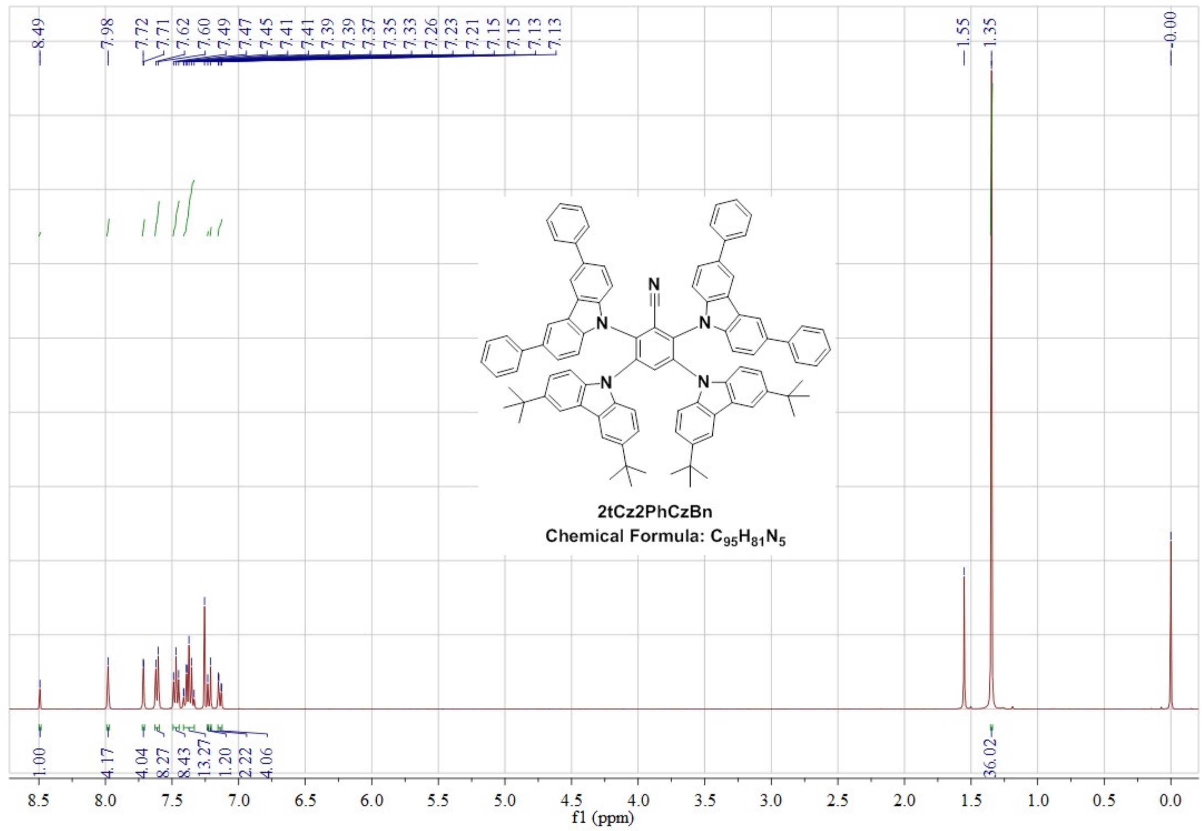


**Figure S7.** $^1$H NMR spectrum of 2tCz2PhCzBn.

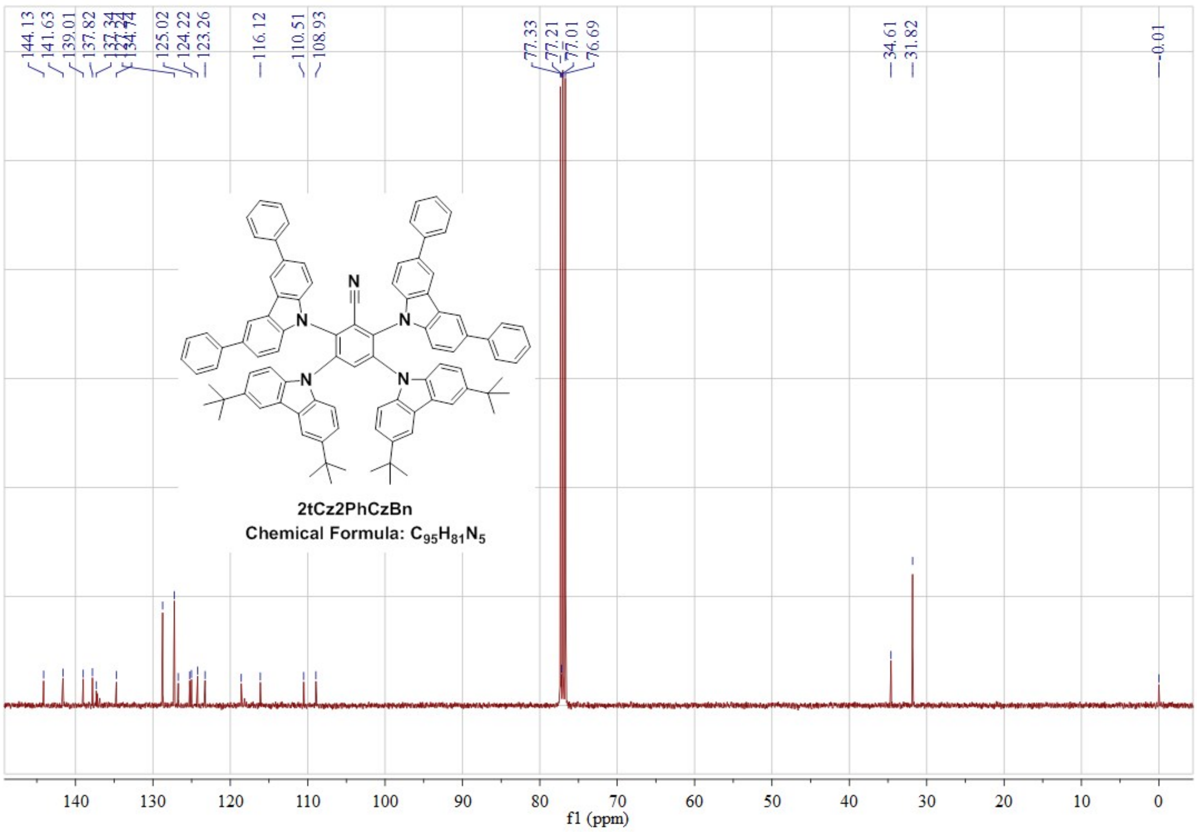


**Figure S8.** $^{13}$C NMR spectrum of 2tCz2PhCzBn.

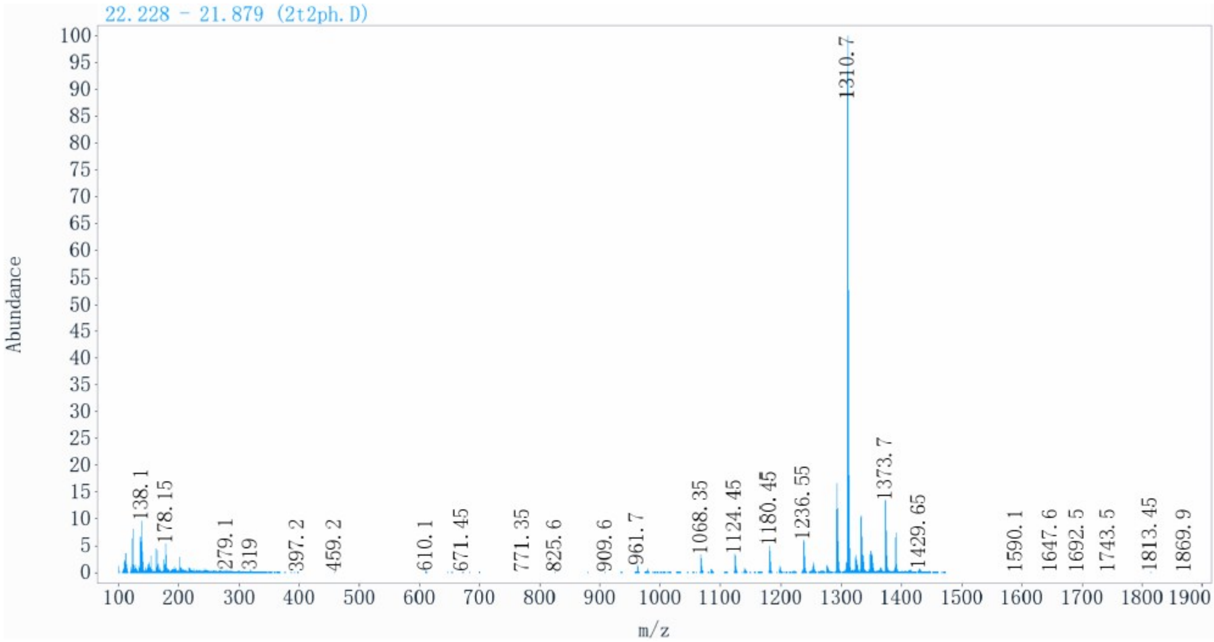


**Figure S9.** TOF-MS spectrum of 2tCz2PhCzBn.

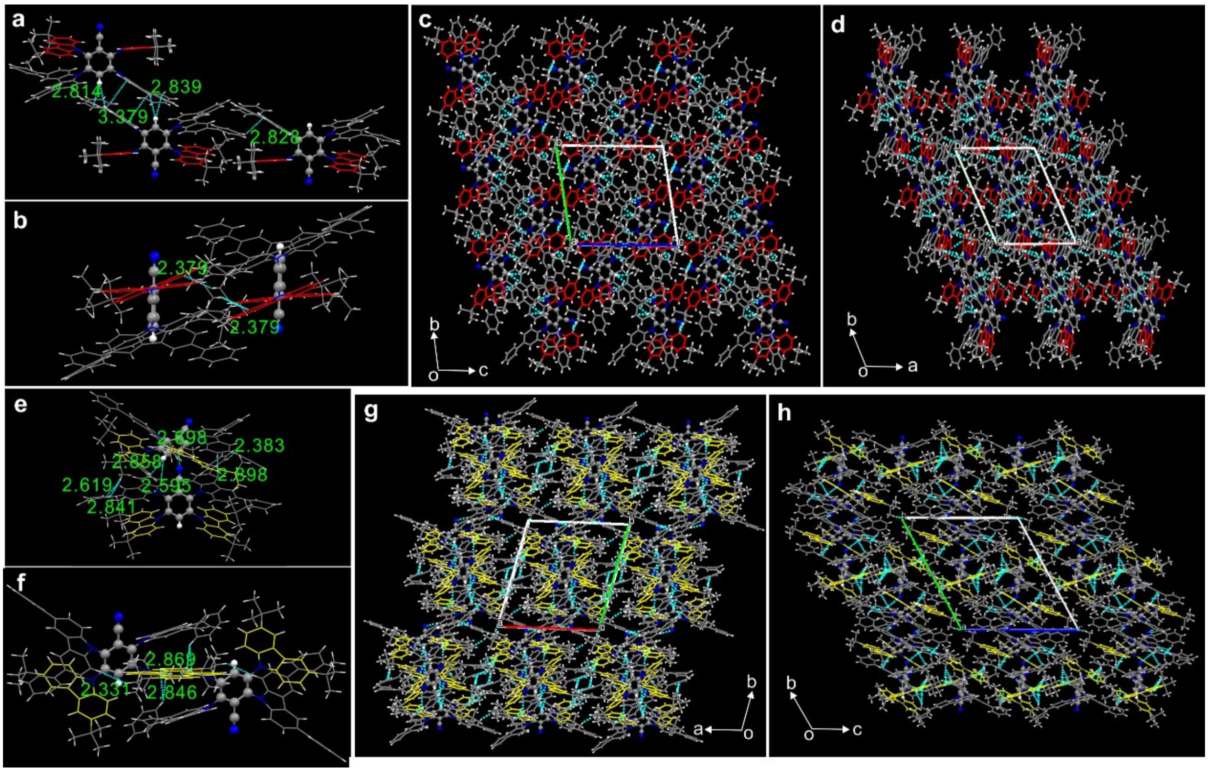


**Figure S10**. Single-crystal structures and molecular packing with selected intermolecular distances of (a-d) **2PhCz2tCzBn** and (e-h) **2tCz2PhCzBn**.

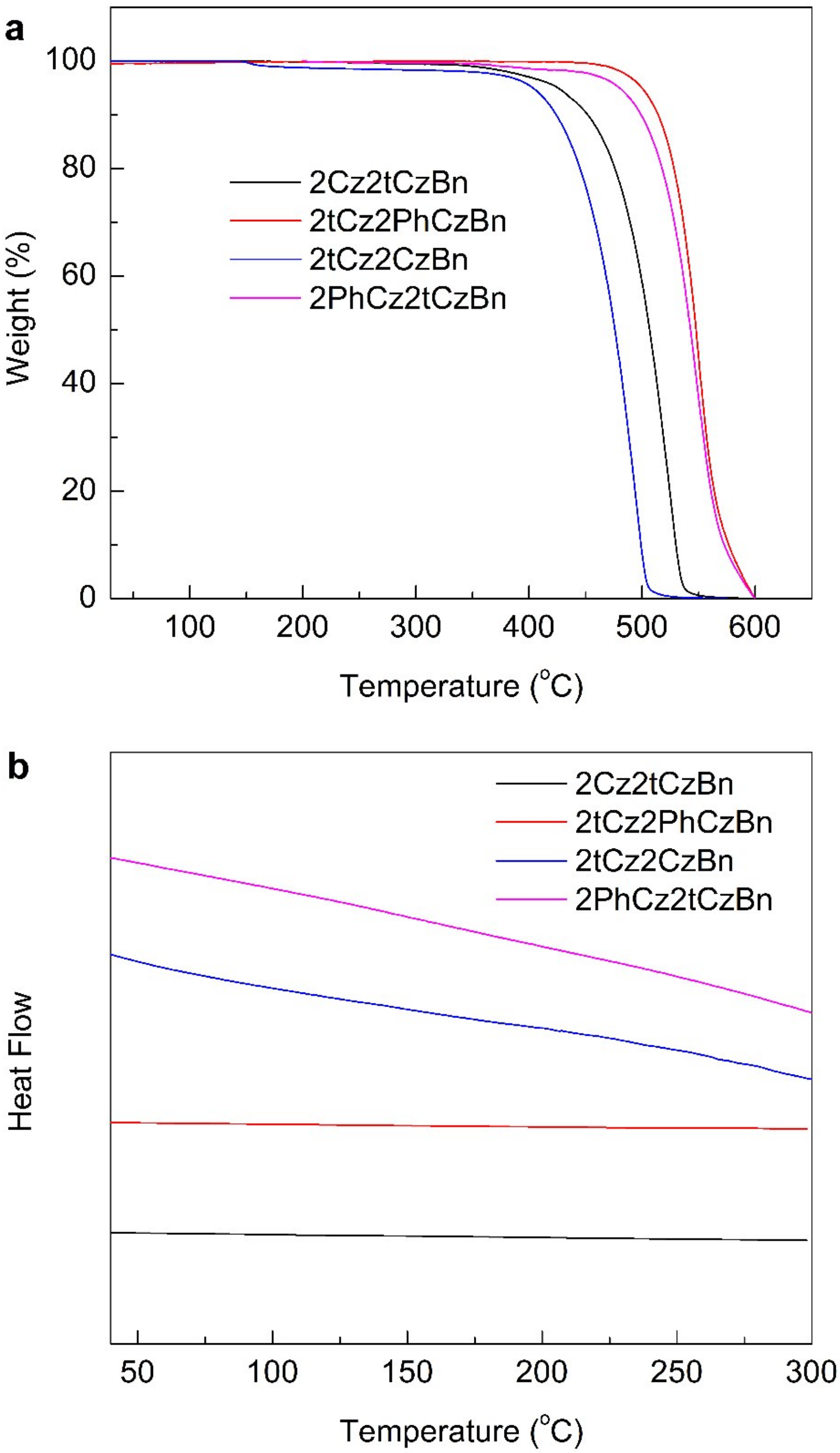


**Figure S11**. (a) TGA and (b) DSC curves of **2Cz2tCzBn**, **2tCz2CzBn**, **2PhCz2tCzBn**, and **2tCz2PhCzBn**.

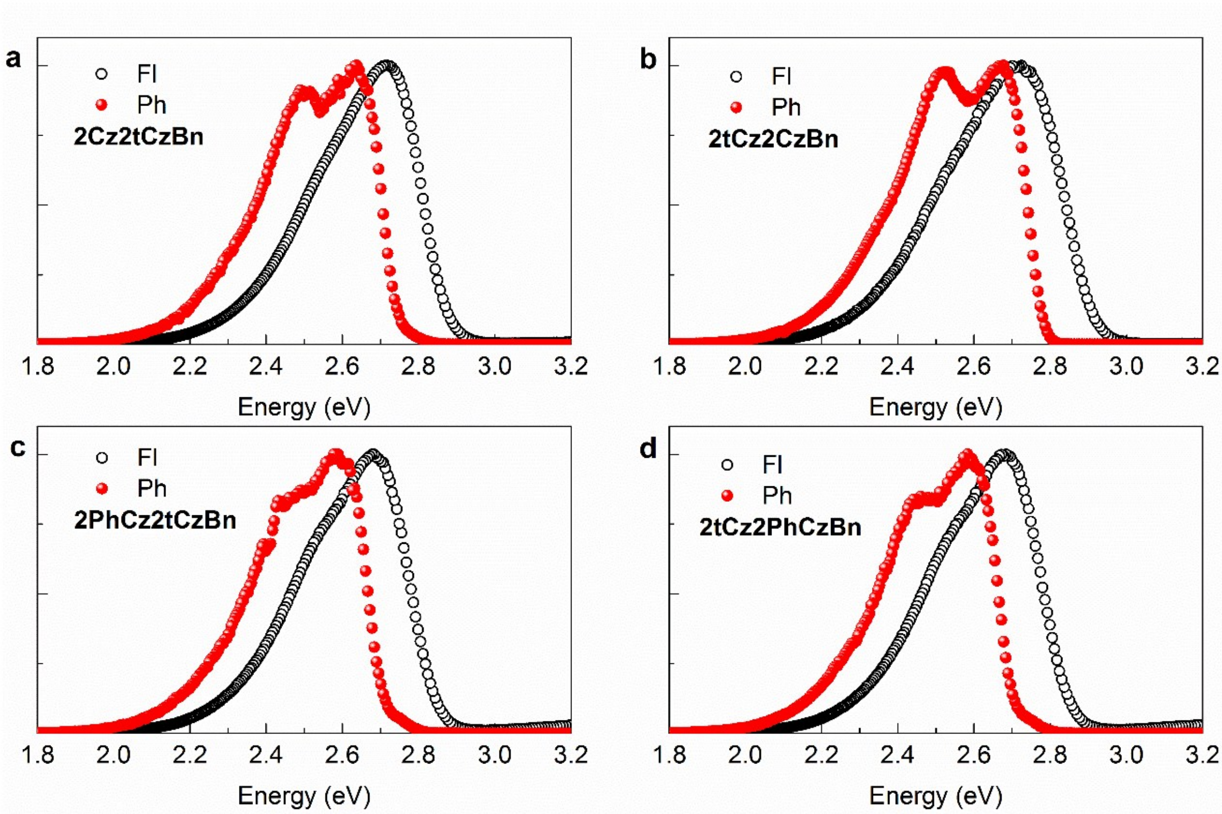


**Figure S 12.** Room-temperature fluorescence and low-temperature phosphorescence (at 77 K) spectra of **2Cz2tCzBn**, **2tCz2CzBn**, **2PhCz2tCzBn**, and **2tCz2PhCzBn**. The $\Delta E_{ST}$ values are estimated from the difference in the threshold energies of two spectra.

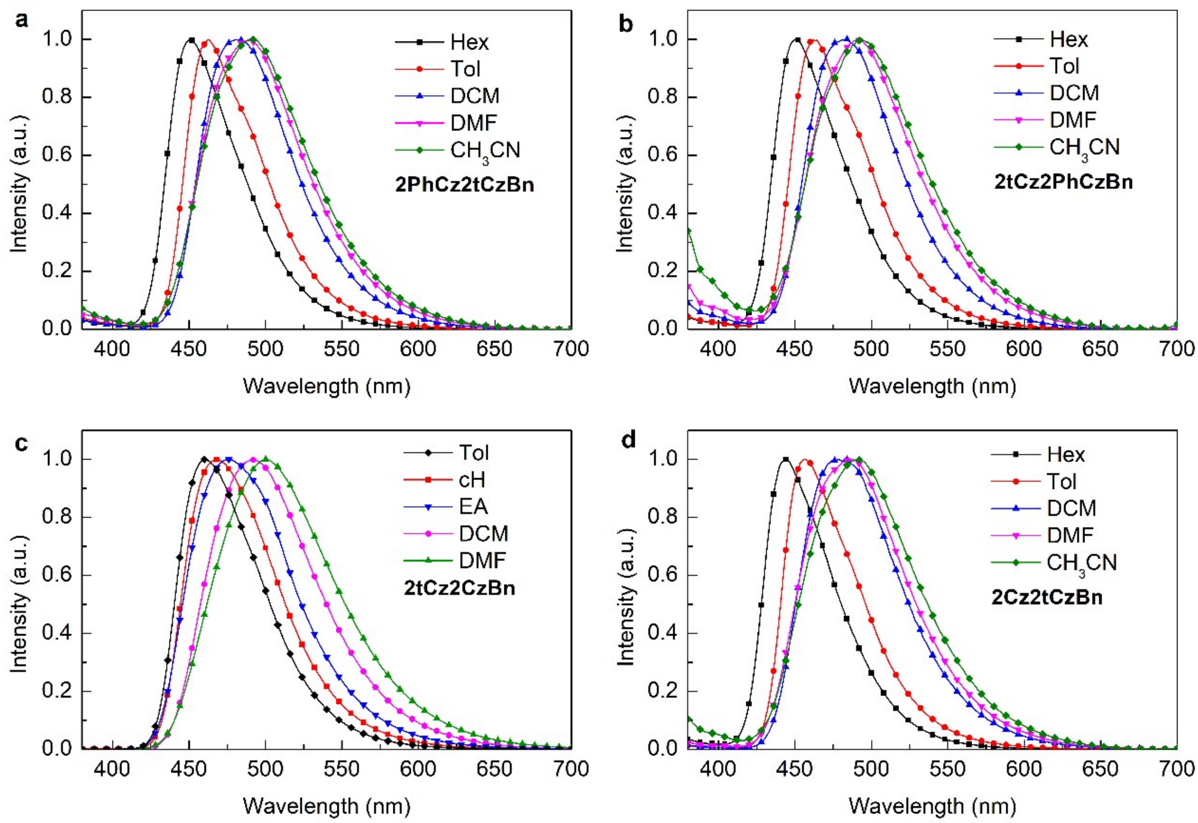


**Figure S13**. PL spectra of (a) **2PhCz2tCzBn**, (b) **2tCz2PhCzBn**, (c) **2tCz2CzBn**, and (d) **2Cz2tCzBn** in different solvents.

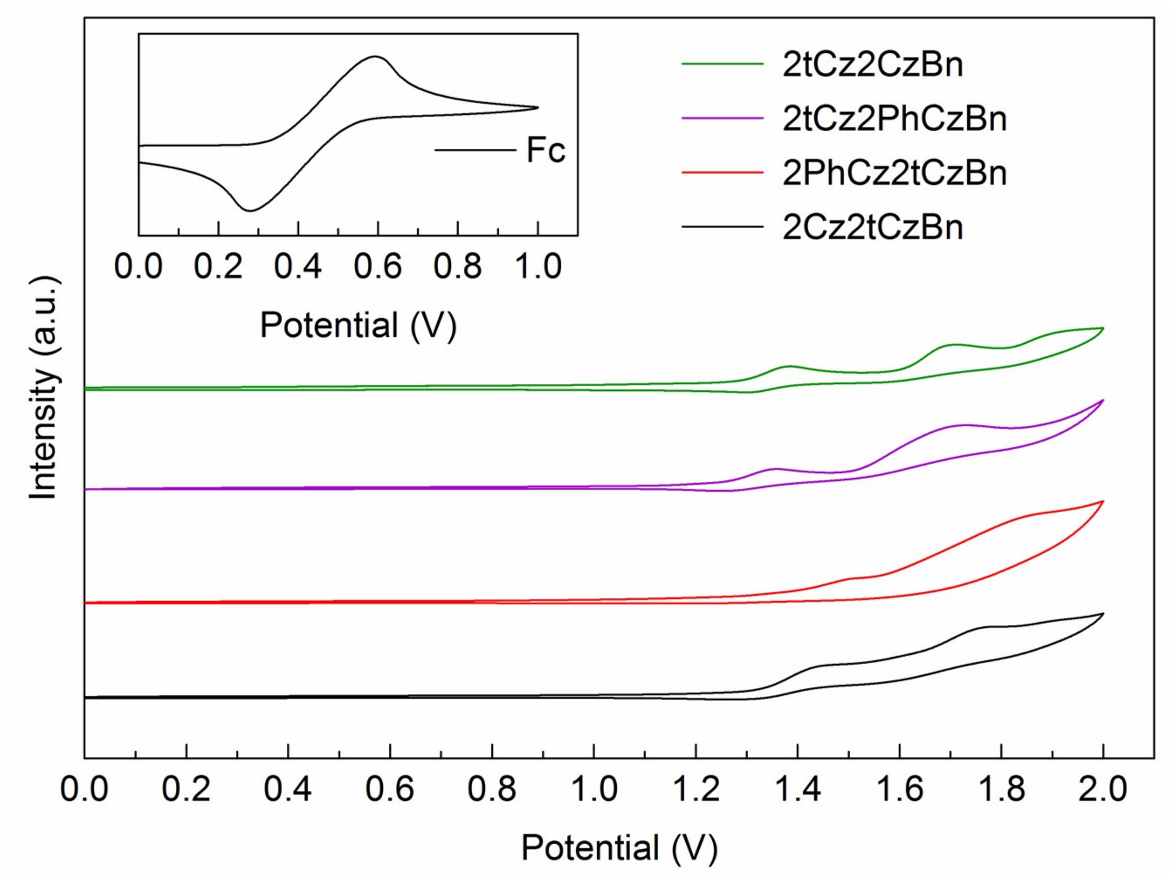


**Figure S14**. Cyclic voltammograms of **2Cz2tCzBn**, **2tCz2CzBn**, **2PhCz2tCzBn**, and **2tCz2PhCzBn** in DCM solution ($10^{-5}$ M).

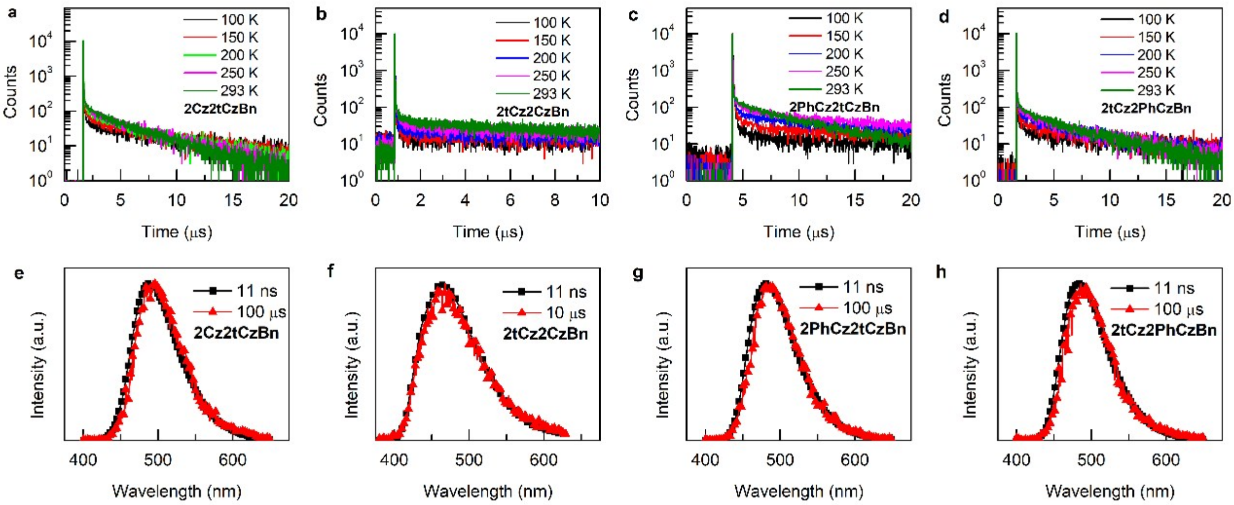


**Figure S15**. (a-d) Temperature-dependent transient PL decay curves of (a) **2Cz2tCzBn**, (b) **2tCz2CzBn**, (c) **2PhCz2tCzBn**, and (d) **2tCz2PhCzBn** in neat films at temperatures ranging from 100 K to 293 K. (e-h) Prompt and delayed emission spectra of (e) **2Cz2tCzBn**, (f) **2tCz2CzBn**, (g) **2PhCz2tCzBn**, and (h) **2tCz2PhCzBn**.

**Table S1.** Photophysical characteristics of four compounds in neat films.

| Films | $\tau_p$ [ns] | $\tau_d$ [μs] | PLQY/$\Phi$p/$\Phi_d$ [%] | $k_r$ [$10^7$ $s^{-1}$] | $k_{ISC}$ [$10^7$ $s^{-1}$] | $k_{RISC}$ [$10^5$ $s^{-1}$] |
|---|---|---|---|---|---|---|
| **2Cz2tCzBn** | 26 | 3.9 | 78/42/36 | 1.6 | 1.8 | 4.7 |
| **2tCz2CzBn** | 10 | 15.7 | 66/31/35 | 2.0 | 3.1 | 3.4 |
| **2PhCz2tCzBn** | 16 | 5.7 | 55/27/28 | 1.6 | 3.2 | 3.3 |
| **2tCz2PhCzBn** | 16 | 5.6 | 53/28/25 | 1.7 | 3.0 | 4.2 |

[1] Radiative rate constants of $S_1$, $k_r = \Phi_p/\tau_p + \Phi_d/\tau_d$.

[2] Nonradiative rate constants of $S_1$, $k_{nr} = k_r(1 - \Phi_{PL})/\Phi_{PL}$.

[3] Rate constants for ISC ($S_1 \rightarrow T_1$), $k_{ISC} = k_p - k_r - k_{nr}$.

[4] Rate constants for RISC ($T_1 \rightarrow S_1$), $k_{RISC} = k_p k_d / k_{ISC} \cdot \Phi_d/\Phi_p$.

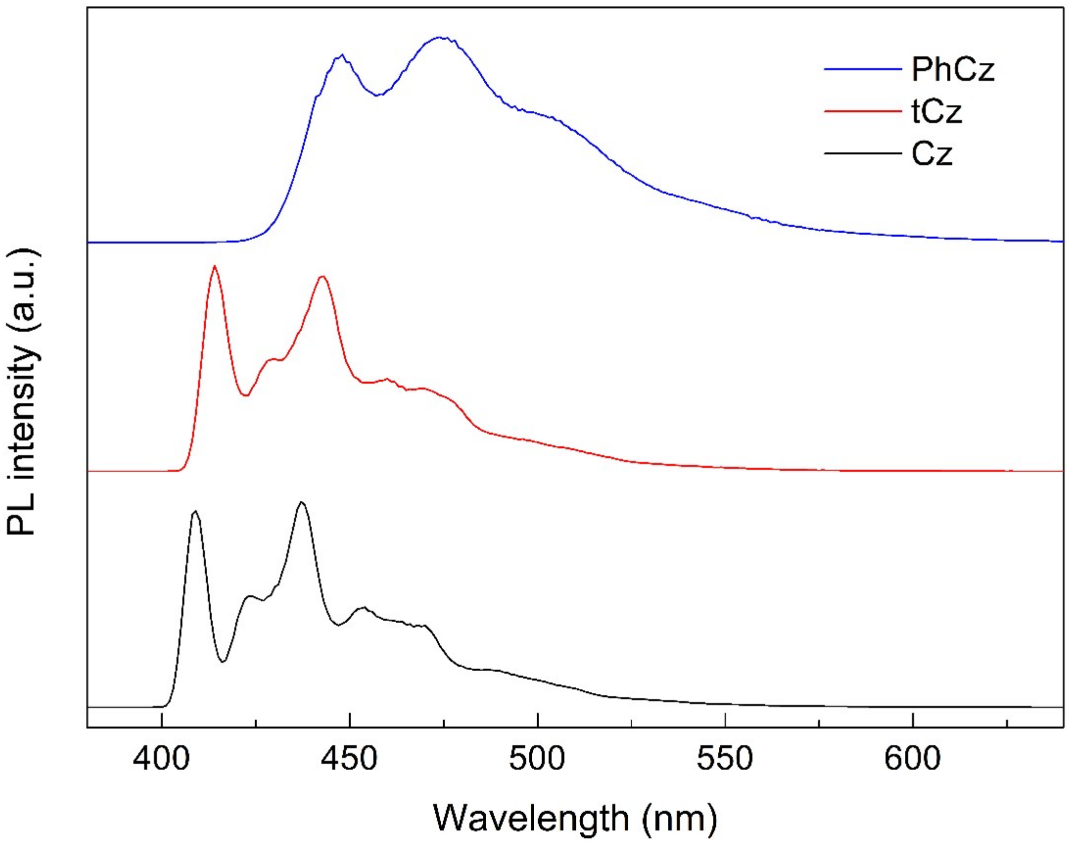


**Figure S16**. Phosphorescence spectra of Cz, tCz and PhCz in toluene at 77 K.

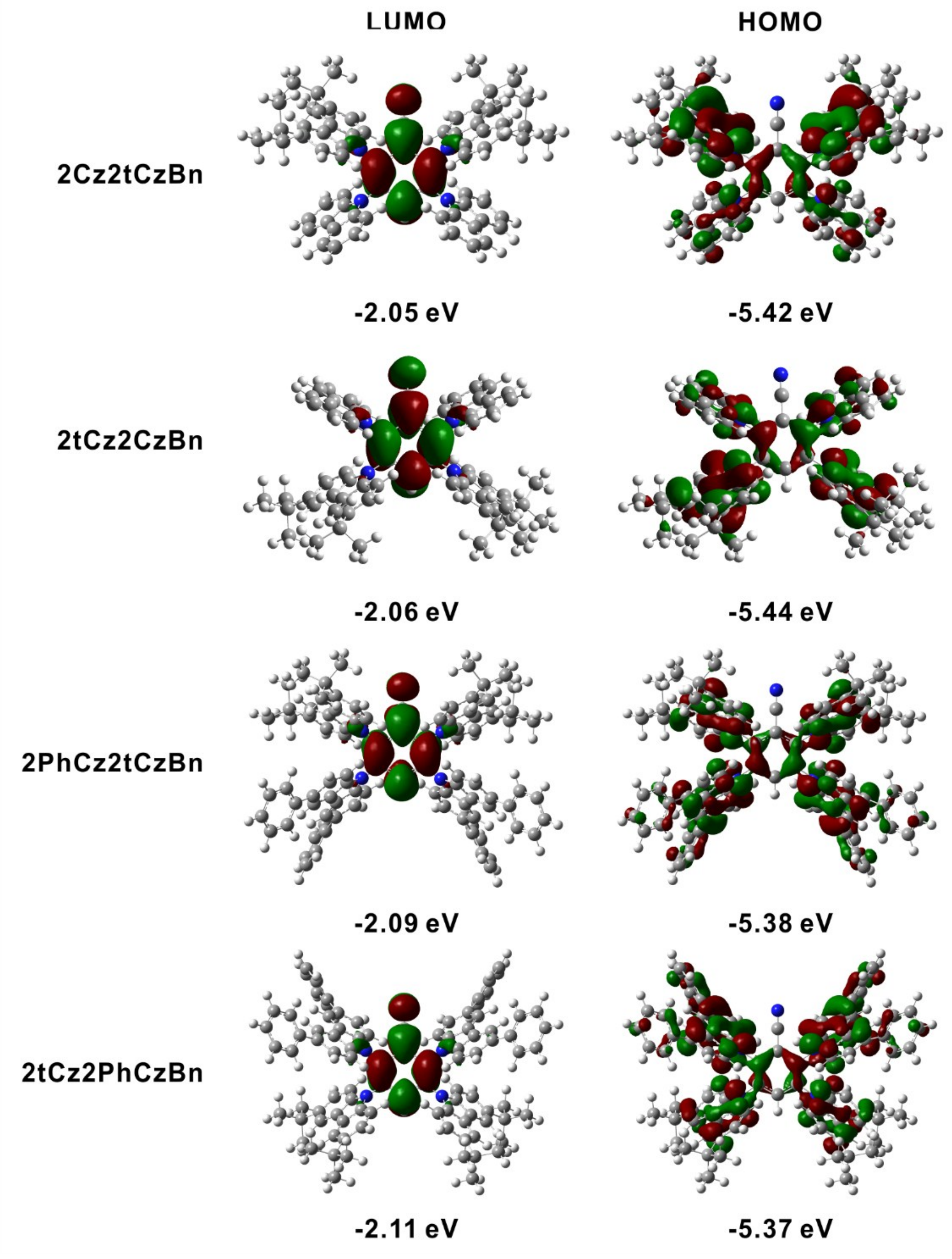


**Figure S17.** Calculated LUMO and HOMO distributions and energy levels of **2Cz2tCzBn**, **2tCz2CzBn**, **2PhCz2tCzBn**, and **2tCz2PhCzBn**.

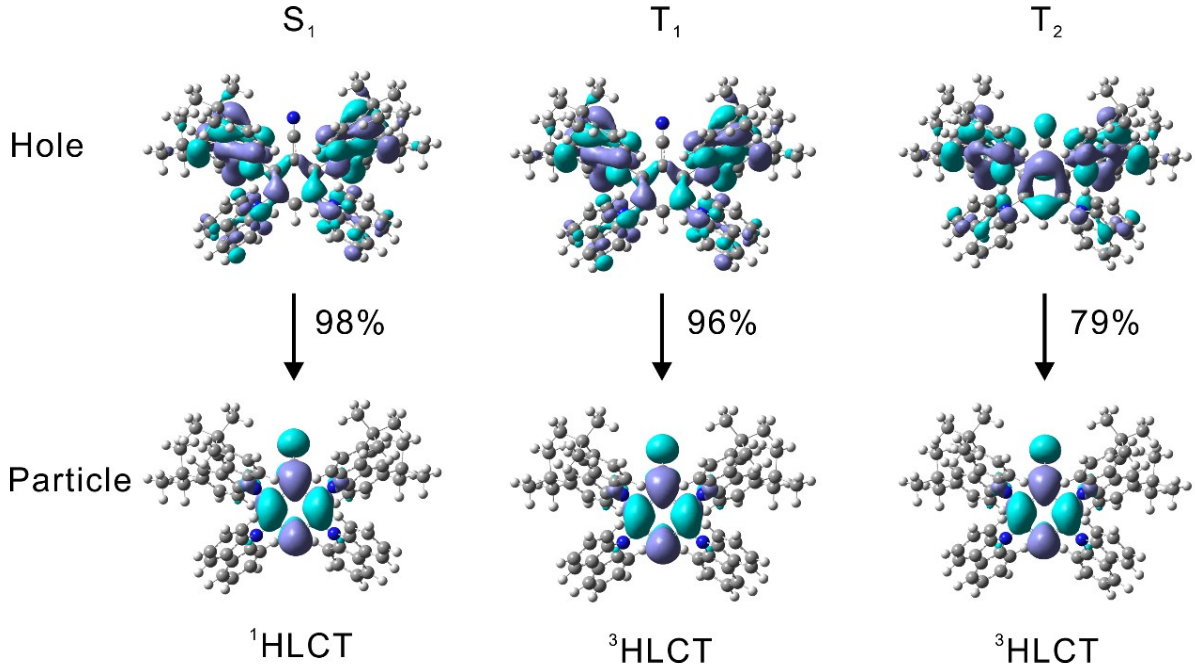


**Figure S18**. Natural transition orbital (NTO) analysis for **2Cz2tCzBn**.

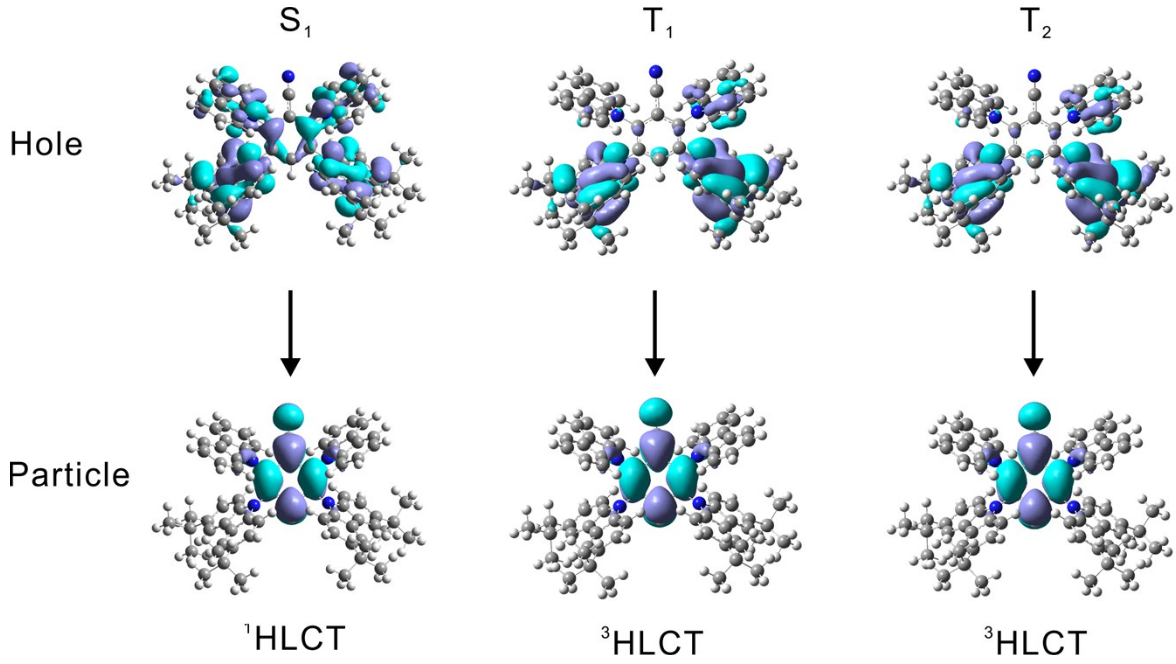


**Figure S19**. Natural transition orbital (NTO) analysis for **2tCz2CzBn**.

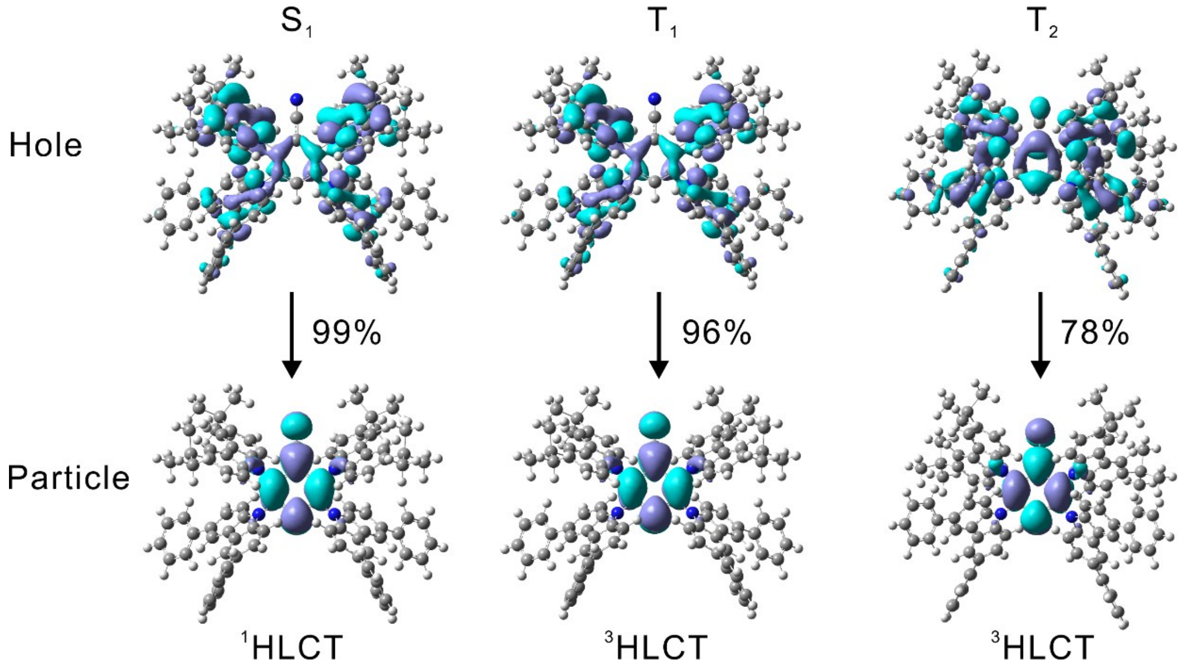


**Figure S20**. Natural transition orbital (NTO) analysis for **2PhCz2tCzBn**.

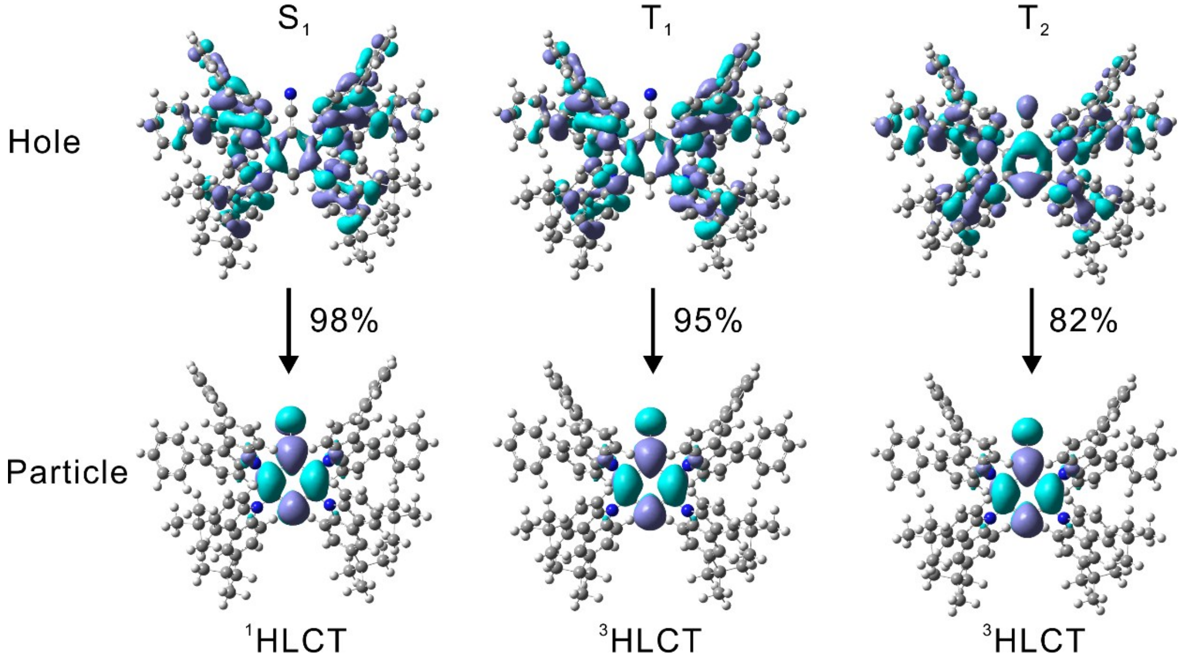


**Figure S21**. Natural transition orbital (NTO) analysis for **2tCz2PhCzBn**.

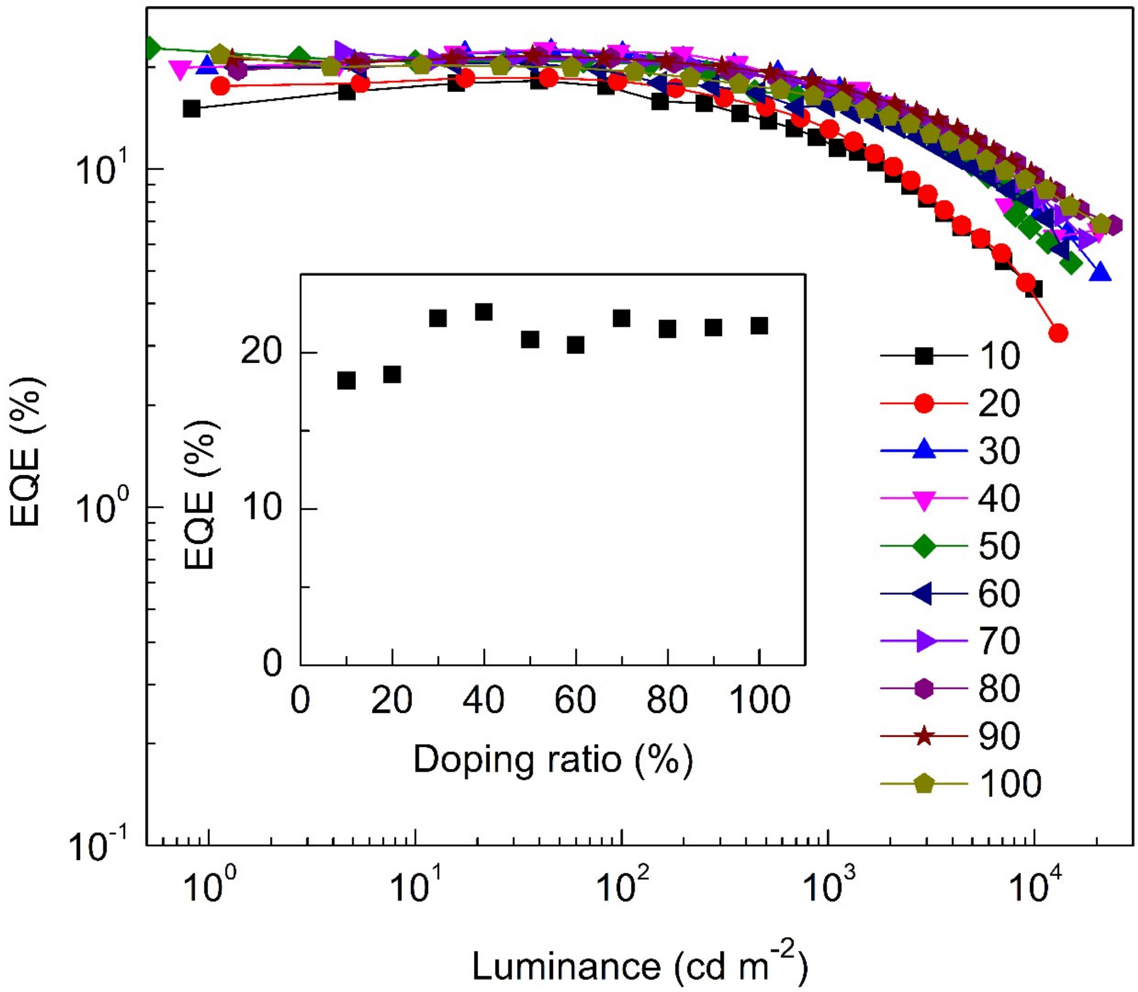


**Figure S22**. EQE evolution of blue OLEDs based on **2Cz2tCzBn** with varied doping concentrations from 10 to 100 wt%. Device structure: ITO/HATCN (10 nm)/TAPC (40 nm)/mCP (10 nm)/mCP:**2Cz2tCzBn** (x wt%, 30 nm)/PO-T2T (50 nm)/LiF (1 nm)/Al (100 nm).

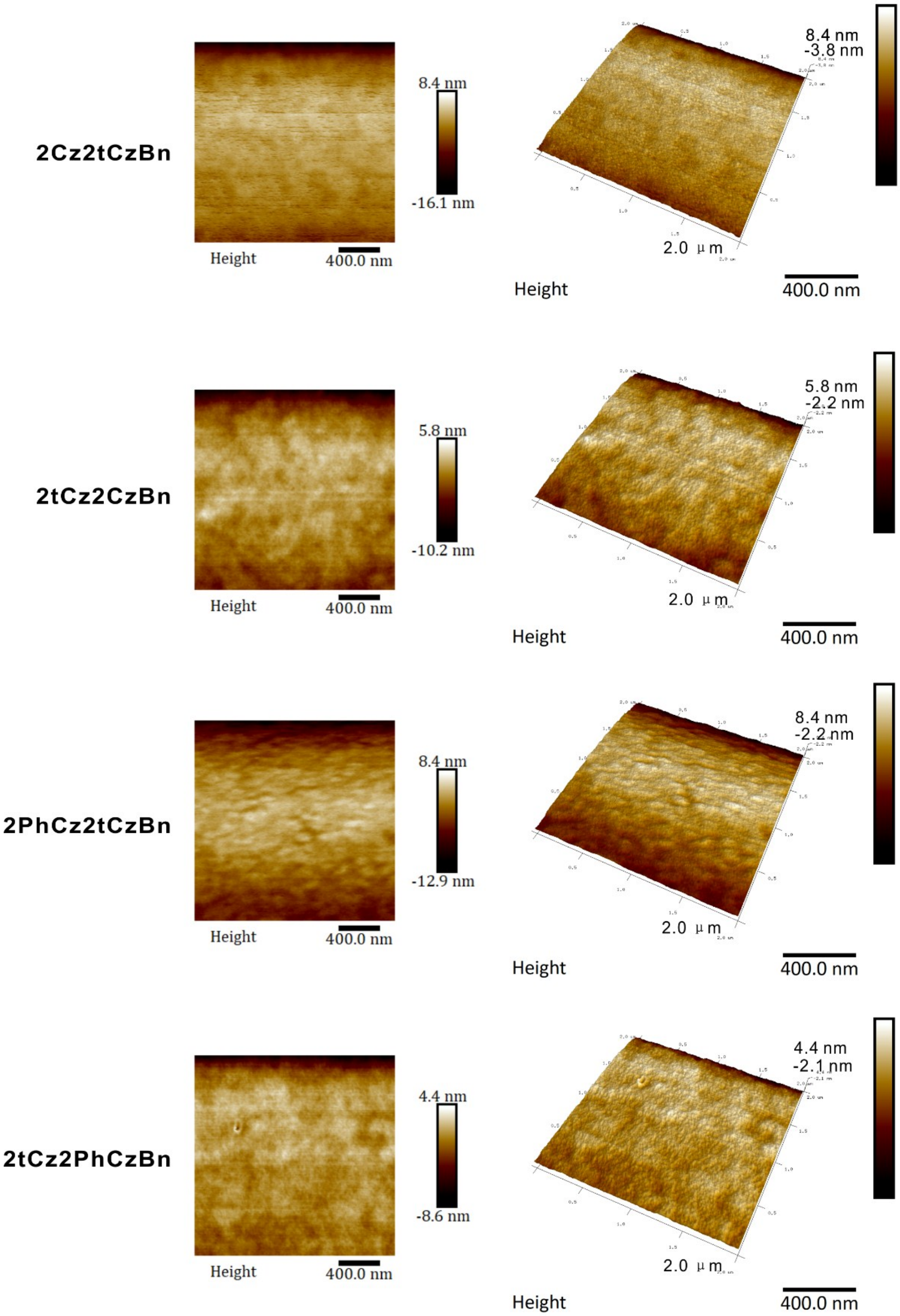


**Figure S23.** AFM images of solution-processed TADF thin films on PVK substrates for (a) **2Cz2tCzBn**, (b) **2tCz2CzBn**, (c) **2PhCz2tCzBn**, and (d) **2tCz2PhCzBn**, respectively.

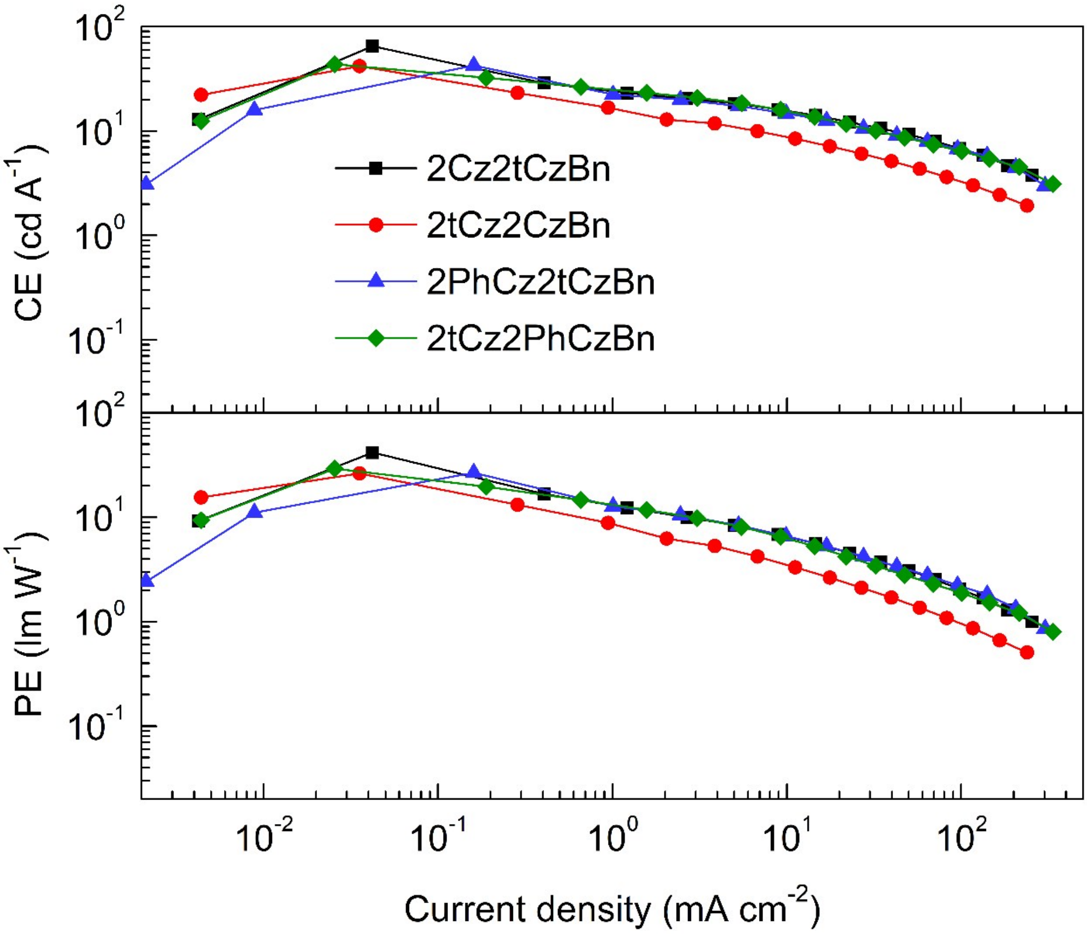


**Figure S24**. Current efficiency (CE) and power efficiency (PE) as a function of current density for solution-processed non-doped blue OLEDs using **2Cz2tCzBn**, **2tCz2CzBn**, **2PhCz2tCzBn**, and **2tCz2PhCzBn**, respectively.

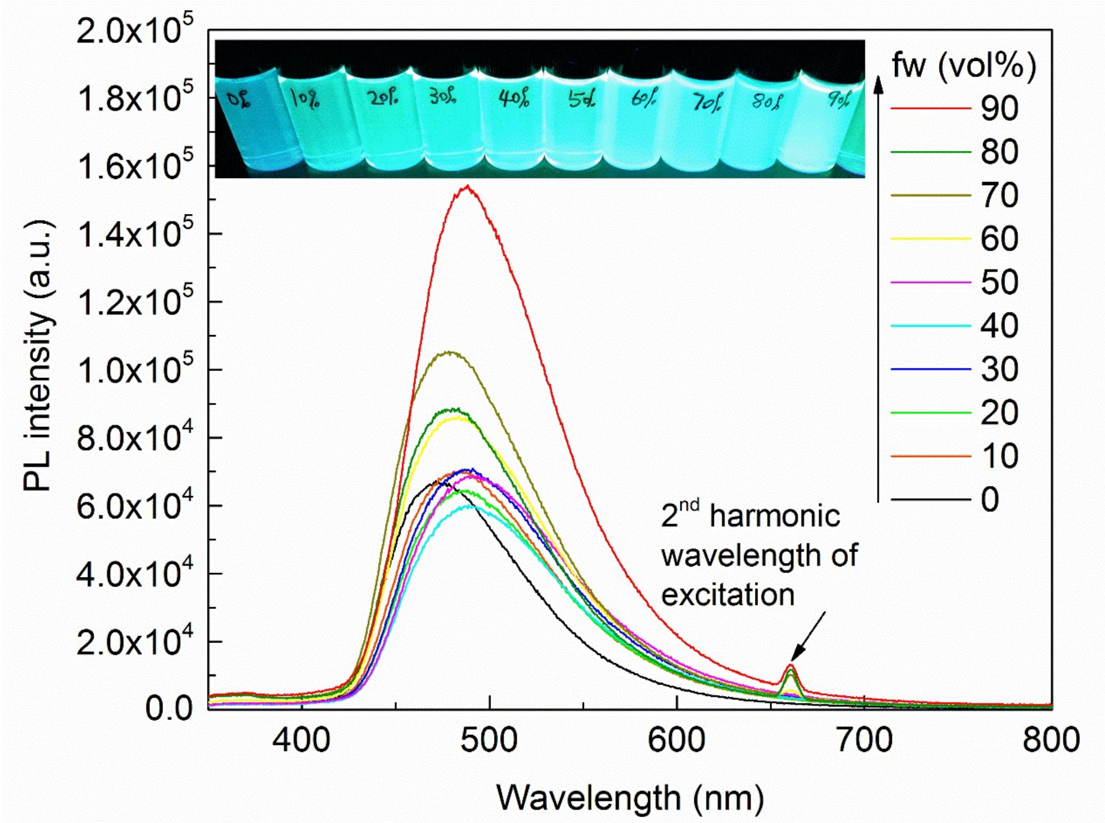


**Figure S25.** PL emission of 2Cz2tCzBn in in THF/water mixtures with different water fractions ($f_w$).

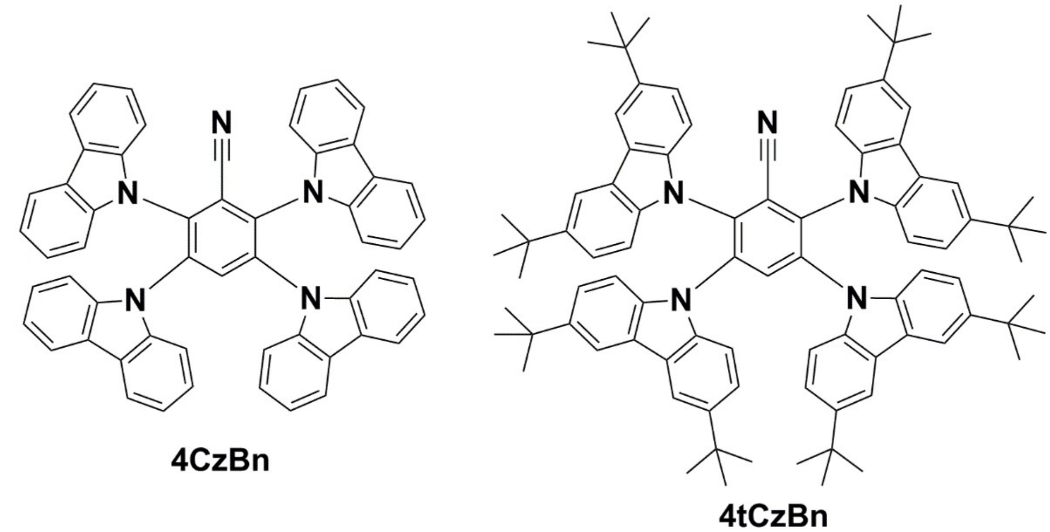


**Scheme S2.** Chemical structures of 4CzBn and 4tCzBn.

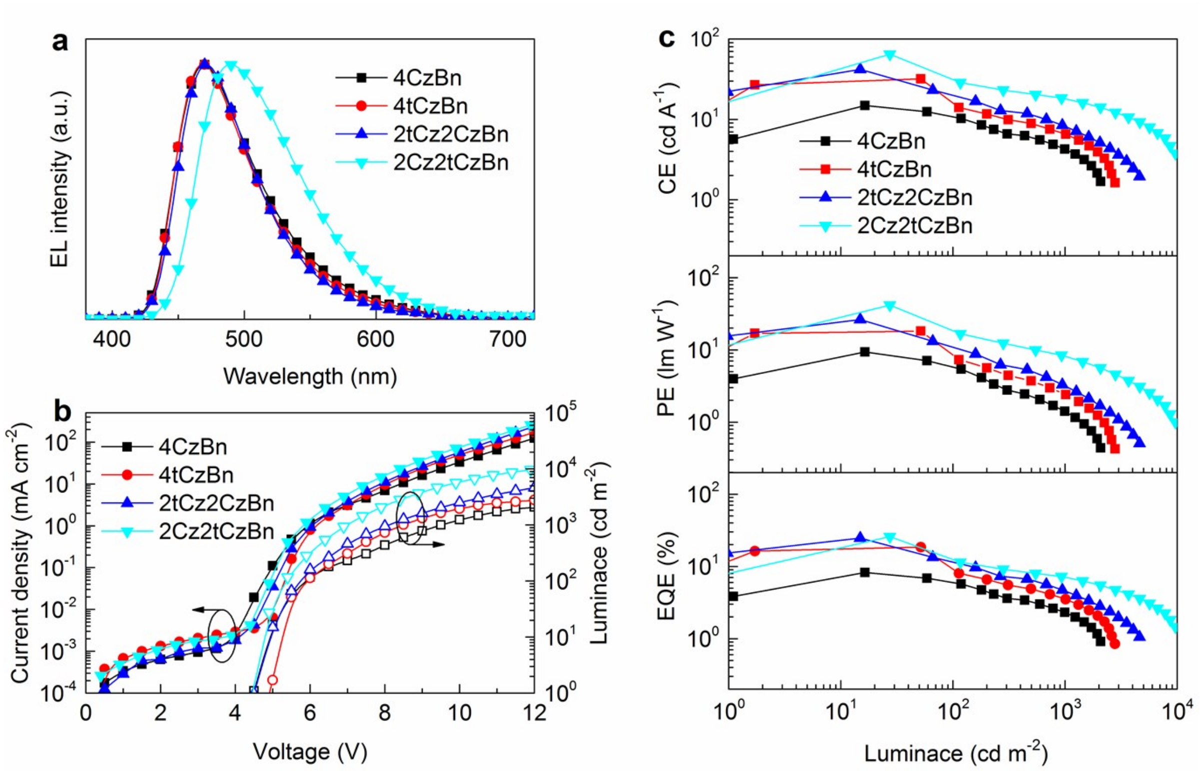


**Figure S26**. (a) EL spectra, (b) current density (J)-voltage (V)-luminance (L) characteristics, and (c) efficiency versus luminance relationships of the nondoped devices.

Two molecules 4CzBn and 4tCzBn have been synthesized (see **Scheme S2**). The EQEs of non-doped devices with 4CzBn and 4tCzBn are 8.2% and 18.4%, respectively. These results fully prove that the tert-butyl substitution is the main factor for the suppressed ACQ.

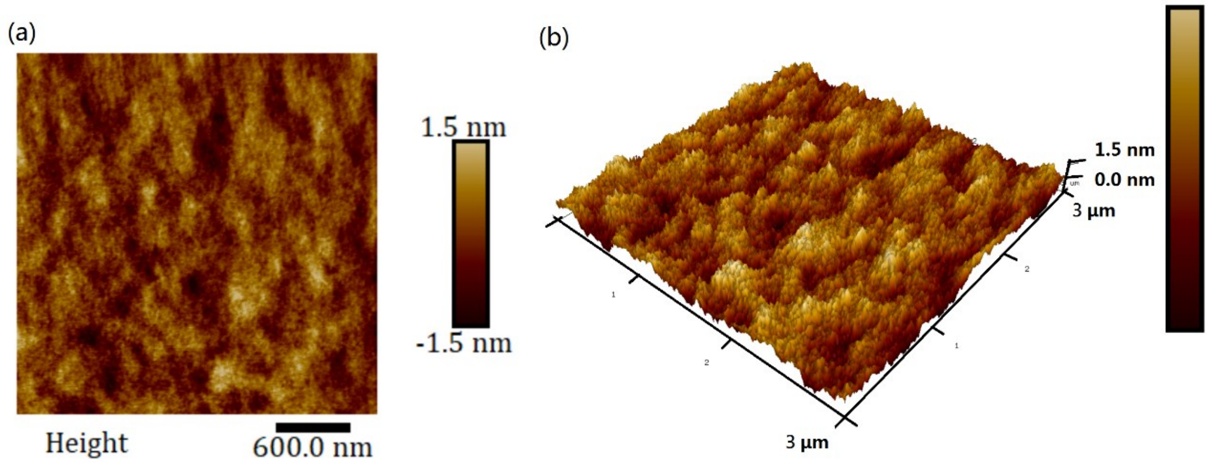


**Figure S27.** AFM images of solution-processed **2tCz2CzBn**:3DMAC-BP thin film on PVK substrate.

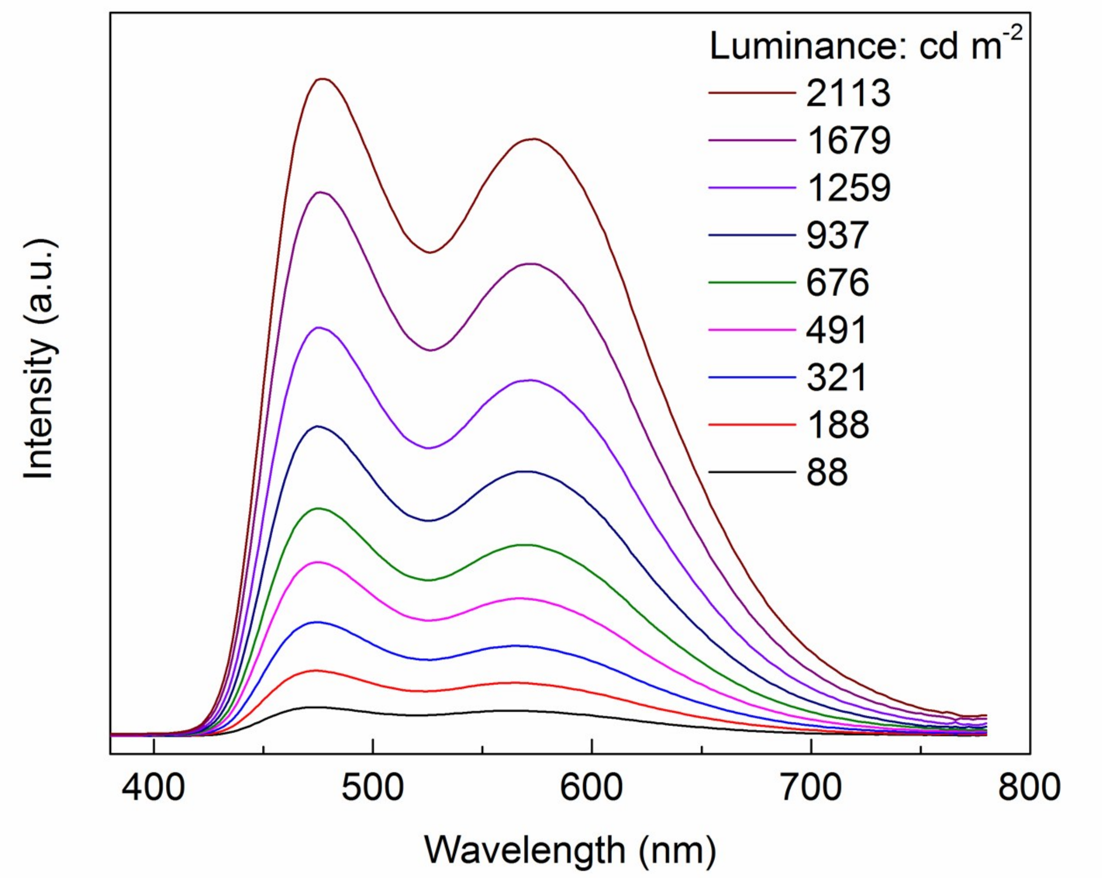


**Figure S28**. EL spectra of white OLED at different luminances.

**Table S2.** Comparison of the representative solution-processed white TADF emitters reported in the literature.

| EML | CIE (x, y) | $CE_{max}$ [cd $A^{-1}$] | $PE_{max}$ [lm $W^{-1}$] | $EQE_{max}$ [%] | Refs |
|---|---|---|---|---|---|
| **2tCz2CzBn:3DMAC-BP** | (0.34, 0.40) | 67.0 | 35.1 | 27.3 | This work |
| **DMAC-TRZ:Ir(dpm)$PQ_2$:PO-01-TB** | (0.35, 0.44) | 48.7 | 44.5 | 17.4 | 39 |
| **PDTPT-1** | (0.31, 0.39) | 38.8 | 20.3 | 14.2 | 40 |
| **DCzDCN:SimCP2:TXO-TPA** | (0.35, 0.39) | 36.50 | 37.31 | 13.39 | 41 |
| **tBuCN-FIrpic-mCP:(m-$CF_3$DPQ)$_2$Ir(pic)** | (0.35, 0.35) | 43.5 | 15.7 | 20.6 | 5 |
| **G2:Ir(bt)$_2$(acac)** | (0.32, 0.33) | 17.69 | 7.88 | 10.1 | 41 |